SEISMIC DESIGN OF SHEAR-TYPE BUILDINGS WITH MAXWELL MODEL-BASED NONLINEAR DAMPER-BRACE SYSTEMS

S. Li[(1)], Y.T. Chen[(2)]

[(1)] *PhD student, University of Nottingham Ningbo China, Siyuan.Li@nottingham.edu.cn*
[(2)] *Associate Professor, University of Nottingham Ningbo China, Yung-Tsang.Chen@nottingham.edu.cn*

Abstract

In this paper, a procedure to design a shear-type building with supplementary Maxwell model-based nonlinear damper-brace systems for achieving a target performance is proposed. In the proposed procedure, a numerical time-stepping method is developed to compute the response of the damper-brace system and the building under earthquake excitations. The effects of different design parameters have been preliminary investigated by a simple structure with a nonlinear damper-brace assembly. Results indicate that, to satisfy a set performance index, there exist non-unique solutions with many possible combinations of the design parameters; however, a minimum brace stiffness will be required to achieve the desired structural performance. Moreover, for a given brace stiffness, the optimal damping coefficient can be uniquely determined if the nonlinear velocity exponent is preset. Results also show that, for achieving the same structural performance, the use of a nonlinear damper with velocity exponent less than 1 can reduce a considerable amount of damping originally required for the use of a linear damper. The proposed procedure will be shown to be easily extendable to multi-degree-of-freedom (MDOF) structures with multiple nonlinear damper-brace systems.

Keywords: seismic design, nonlinear fluid viscous damper, brace stiffness, Maxwell model, optimal design.

1. Introduction

As a typical structural protective technique, passive energy dissipation is now widely used in civil engineering structures to improve overall structural performance, which may include vibration control and retrofit of the structures. High performance passive energy dissipating devices, such as friction dampers, viscous dampers, viscoelastic dampers, tuned mass dampers and tuned liquid dampers, can consume or absorb part of the energy that is imparted to the primary structure, and thereby reducing the dynamic actions on structural elements [1]. Among the many passive control devices, fluid viscous dampers (FVDs), which were initially applied in aerospace and military hardware, are frequently adopted in civil engineering to mitigate structural vibration due to natural and man-made excitations. If properly designed, a supplementary FVD system can dissipate a significant amount of energy imparted to a structure from earthquakes and wind, thus enhance the dynamic performance of the structure.

FVDs can generally be categorized into two groups according to their force-velocity relationships, namely linear and nonlinear. While extensive researches have been focused on linear FVDs experimentally and analytically [2-5], studies in 'nonlinear FVDs', which have an additional velocity exponent that introduces the nonlinear power-law behavior, are still limited and requires further investigation. The damping force in the nonlinear damper can be described as:

$$f_d^{NL} = c_d \left|\dot{\Delta}_d\right|^{\nu} \operatorname{sgn}(\dot{\Delta}_d) \tag{1}$$

where f_d^{NL} is the nonlinear force induced by the damper, c_d is the damping coefficient, $\dot{\Delta}_d$ is the relative velocity between two ends of the damper, namely, the piston velocity, ν is the nonlinear velocity exponent and sgn(•) is the signum function. The exponent ν contributes to the nonlinearity of the damper and depends on the hydraulic circuit (orifice) design of the device [6]. For seismic applications, typical values of ν are in the range of 0.35−1.0 [7] and the values commonly used are in the range of 0.4−0.5 [8]. For wind applications, the frequently used velocity exponent is in the range of 0.5−1.0 [8].

Compare with linear FVDs, nonlinear FVDs with a velocity exponent ν smaller than 1 are capable of providing sufficient damping to the structure without creating excessive damper force when the structural velocities are large [7]. This can be demonstrated by Fig. 1, which shows that the nonlinear damper with a ν less than 1 can generate a larger damper force at velocity lower than 1 m/s. It can also be seen from Fig. 1 that, when the velocity is larger than 1 m/s, the force provided by the damper with ν equals 0.3 shows a diminishing return, unlike a linear increase (for ν equals 1) or an exponential increase (for ν equals 1.5). The damper force can thus be limited, and possible structural/joint damage due to large damper force can be prevented. Owing to the afore-mentioned advantages provided by the nonlinear FVDs with ν smaller than 1, the use of nonlinear FVDs in structural applications becomes an active area of research in recent years [6, 7].

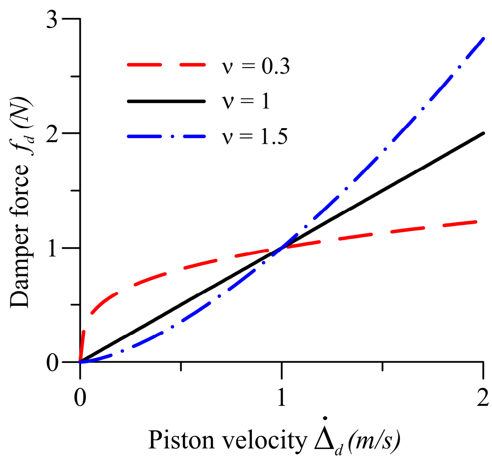

Fig. 1 – Variation of damper force with piston velocity for different damper exponents (c_d = 1 N·s/m)

In practice, FVDs are often installed in buildings in conjunction with supporting braces, which may be of Chevron (Inverted-V), diagonal, or other types of configuration. Since the dampers are connected to the braces, for FVDs to exhibit optimal performance, it is vital that the effect of the braces to be considered in the design of the dampers. However, in the literature, most of the design procedures for FVDs, especially the procedures for nonlinear ones, assume the supporting braces have infinite stiffness [6, 9-12], as the brace stiffness has not yet been included as a design parameter. Since in practical application, the cross-section of the brace is often limited due to functional or aesthetic reasons, an infinite stiffness is difficult to achieve [13]; hence, researchers have suggested that the brace stiffness should be considered throughout the design of damper properties and positioning [13-15]. Due to the fact that the FVDs are often arranged in series with the braces, in mathematical term, the damper-brace assembly can best be described using the Maxwell model, in which the damper, represented by a dashpot, and the brace, represented by a spring, are in series.

For structures with damper-brace systems described by the Maxwell models to achieve the best performance, some design procedures have been introduced in the literature, e.g. Londoño et al. [16] proposed a design method for linear damper-brace systems in single-degree-of-freedom (SDOF) structures to determine the minimum brace stiffness or the minimum damping coefficient to achieve a target damping ratio of the system. Chen and Chai [17] have conducted an in-depth research focusing on the effects of supporting brace on the effectiveness of linear FVDs and the overall structural performance. To investigate the behavior of damper-brace systems with nonlinear elements, Lu et al. [18] proposed a Generalized Maxwell Model, in which the linear stiffness and damping elements are replaced by the nonlinear ones. Despite the research work conducted mentioned above, a thorough study about the effect of brace stiffness on the performance of nonlinear FVDs has not been carried out.

Performance-based design has been widely recognized as an ideal framework for seismic design; in this design philosophy, the design criteria are set based on achieving specified performance objectives. Following the concept of performance-based design, the improved performance can be examined in terms of response reduction, e.g. displacement, acceleration, base shear and inter-story drift. For buildings with supplemental braces and nonlinear dampers, a response reduction can be achieved by a suitable and strategic combination of brace stiffness, damping coefficient and velocity exponent of the damper-brace systems, rather than relying on dampers alone as conventionally been done. In this paper, a procedure to design a shear building with Maxwell model-based nonlinear damper-brace systems for satisfying a certain performance level is proposed; the effects of different design parameters on the structural performance, especially the brace stiffness and the nonlinear velocity exponent of FVD, are analyzed and summarized.

2. Analytic model for a SDOF structure with a nonlinear damper-brace system

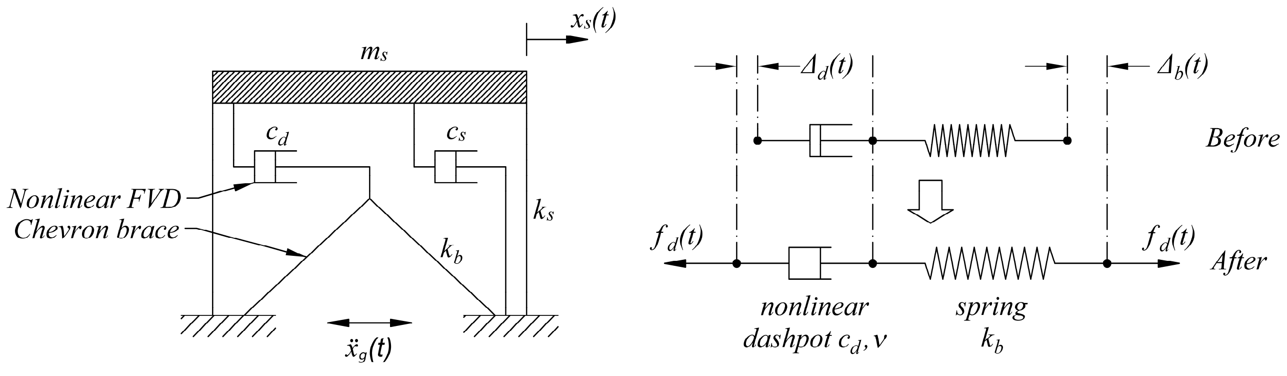

(a) SDOF structure **(b) Maxwell model under loading**

Fig. 2 – (a) Analytical model of a single-story structure with a nonlinear FVD (b) Maxwell model under a external load $f_d(t)$

A SDOF structure with a supplementary nonlinear viscous damper installed on top of a Chevron brace, as shown in Fig. 2(a), is investigated in this section. The serial arrangement of the nonlinear FVD and the brace can be represented by the Maxwell model, as shown in Fig. 2(b). Equation of motion of the SDOF structure under earthquake excitations can be described as:

$$m_s \ddot{x}_s(t) + c_s \dot{x}_s(t) + k_s x_s(t) + f_d(t) = -m_s \ddot{x}_g(t) \tag{2}$$

where m_s, c_s, k_s and $x_s(t)$ are the mass, damping coefficient, lateral stiffness and horizontal displacement of the structure, respectively, $f_d(t)$ is the force provided by the supplementary damper-brace system and $\ddot{x}_g(t)$ is the ground acceleration in the horizontal direction. Since the nonlinear damper and the Chevron brace are connected in series, the damping force in the damper and the restoring force in the brace will be the same. The damping force obeys a nonlinear power law and the restoring force obeys Hooke's law:

$$f_d(t) = k_b \Delta_b(t) = c_d \left|\dot{\Delta}_d(t)\right|^{\nu} \operatorname{sgn}(\dot{\Delta}_d(t)) \tag{3}$$

where k_b and $\Delta_b(t)$ are the horizontal stiffness and deformation of the brace, respectively, c_d and $\dot{\Delta}_d(t)$ are the damping coefficient and deformation rate of the damper, respectively, ν is the exponential of the damper velocity $\dot{\Delta}_d(t)$ and the signum function sgn(•) is defined as:

$$\operatorname{sgn}(x) = \begin{cases} 1 & for\ \ x > 0 \\ 0 & for\ \ x = 0 \\ -1 & for\ \ x < 0 \end{cases} \tag{4}$$

In the Maxwell model shown in Fig. 2(b), the kinematic conditions of the nonlinear damper-brace system can be described as:

$$\Delta(t) = \Delta_d(t) + \Delta_b(t) \tag{5}$$

and

$$\dot{\Delta}(t) = \dot{\Delta}_d(t) + \dot{\Delta}_b(t) \tag{6}$$

where $\Delta(t)$ is the total deformation of the nonlinear damper-brace system.

The following Sections 2.1 and 2.2 will first explain the proposed time-stepping method for calculating the dynamic response of the SDOF structure in Fig. 2(a), followed by expanding the method to simulate the discrete-time state force $f_d[k]$ of the nonlinear damper-brace system.

2.1 Dynamic response of the structure-brace-damper model

The equation of motion in Eq. (2) can be expressed by a first-order differential equation:

$$\dot{\mathbf{z}}(t) = \mathbf{A}^* \mathbf{z}(t) + \mathbf{B}^* f_d(t) + \mathbf{E}^* \ddot{x}_g(t) \tag{7}$$

where $\mathbf{z}(t) = \begin{bmatrix} x_s(t) \\ \dot{x}_s(t) \end{bmatrix}$ is the response vector of the damper-brace system, $\mathbf{A}^* = \begin{bmatrix} 0 & 1 \\ -m_s^{-1}k_s & -m_s^{-1}c_s \end{bmatrix}$ is the system matrix, $\mathbf{B}^* = \begin{bmatrix} 0 \\ -m_s^{-1} \end{bmatrix}$ and $\mathbf{E}^* = \begin{bmatrix} 0 \\ -1 \end{bmatrix}$ are, respectively, the distribution vectors of damper force $f_d(t)$ and ground acceleration $\ddot{x}_g(t)$.

Eq. (7) is the state space model in time domain. The structural response can be further expressed as a discrete-time state function for two consecutive sampling points k and $k + 1$, as:

$$\mathbf{z}[k+1] = \mathbf{A_e} \mathbf{z}[k] + \mathbf{B_e} f_d[k] + \mathbf{E_0} \ddot{x}_g[k] + \mathbf{E_1} \ddot{x}_g[k+1] \tag{8}$$

where:

$\mathbf{A_e} = e^{\mathbf{A}^*\Delta t}$ is the discrete system matrix;

$\mathbf{B_e} = \mathbf{A}^{*^{-1}}(\mathbf{A_e} - \mathbf{I})\mathbf{B}^*$ is the instant discrete force distribution matrix;

$\mathbf{E_0} = \left[\mathbf{A}^{*^{-1}}\mathbf{A_e} + \frac{1}{\Delta t}\mathbf{A}^{*^{-2}}(\mathbf{I} - \mathbf{A_e})\right]\mathbf{E}^*$ is an instant discrete external disturbance matrix;

$\mathbf{E_1} = \left[-\mathbf{A}^{*^{-1}} + \frac{1}{\Delta t}\mathbf{A}^{*^{-2}}(\mathbf{A_e} - \mathbf{I})\right]\mathbf{E}^*$ is an instant discrete external disturbance matrix;

Δt is the sampling period.

It should be noted that in the interval between two consecutive sampling instants, it is assumed that the damper force is piecewise constant, while the external ground acceleration varies linearly in each time step.

2.2 Force in nonlinear damper-brace system

If the damper force $f_d[k]$ is known as a prior, the system's response can be found by Eq. (8); hence, to obtain the damper force, Eq. (3) may be written as:

$$\dot{\Delta}_d(t) = \left(\frac{k_b}{c_d}\right)^{\frac{1}{\nu}} |\Delta_b(t)|^{\frac{1}{\nu}} \tag{9}$$

For a SDOF structure with a damper supported by a Chevron brace shown in Fig. 2(a), the lateral story velocity of the structure is equal to the total deformation rate of the supplementary system, hence Eq. (6) becomes:

$$\dot{x}_s(t) = \dot{\Delta}_d(t) + \dot{\Delta}_b(t) \tag{10}$$

Eq. (10) shows that the relative story velocity of the structure to the ground equals sum of the deformation rates of the damper and the brace. Substitute the expression of $\dot{\Delta}_d(t)$ from Eq. (10) in Eq. (9) yields:

$$\dot{\Delta}_b(t) = A(t)\Delta_b(t) + \dot{x}_s(t) \tag{11}$$

where $A(t)$ changes with the deformation of Chevron brace $\Delta_b(t)$:

$$A(t) = -\left(\frac{k_b}{c_d}\right)^{\frac{1}{\nu}} |\Delta_b(t)|^{\left(\frac{1}{\nu}-1\right)} \tag{12}$$

Since total deformation rate of the nonlinear damper-brace system across the entire time period is not listed in advance, namely, $\dot{x}_s[k+1]$ is unknown in step $[k]$, it is assumed that the coefficient $A(t)$ and the deformation rate $\dot{x}_s(t)$ are piecewise constants between two consecutive sampling instants:

$$\begin{cases} A(\tau) = A(k\Delta t) \\ \dot{x}_s(\tau) = \dot{x}_s(k\Delta t) \end{cases} \quad for\ k\Delta t < \tau < (k+1)\Delta t \tag{13}$$

Take Laplace transform of Eq. (11) yields:

$$\Delta_b(s) = G(s)\Delta_b(t_0) + G(s)\dot{x}_s(s) \tag{14}$$

where $G(s) = [s - A(s)]^{-1}$. Take inverse Laplace Transformation of Eq. (14) and substitute Eq. (13) in the solution, the discrete-time state equation of the brace deformation Δ_b can be expressed as:

$$\Delta_b[k+1] = A_d[k]\Delta_b[k] + A[k]^{-1}(A_d[k] - 1)\dot{x}_s[k] \tag{15}$$

where $A[k] = -(k_b / c_d)^{\frac{1}{v}} \left|\Delta_b[k]\right|^{(\frac{1}{v}-1)}$ and $A_d[k] = e^{A[k]\Delta t}$.

The nonlinear damper and brace force at the sampling instant [k + 1] can then be calculated by substituting the brace deformation $\Delta_b[k + 1]$ in Eq. (15) into Eq. (3):

$$f_d[k+1] = k_b\Delta_b[k+1] = k_b\left[A_d[k]\Delta_b[k] + A[k]^{-1}\left(A_d[k]-1\right)\dot{x}_s[k]\right] \tag{16}$$

The damper force $f_d[k]$ in Eq. (8) can be calculate using Eq. (16). It should be noted that, before an earthquake, the structure should be initially at rest, i.e. $\mathbf{z}[1] = [0 \quad 0]^{\mathrm{T}}$, thus there is no deformation of the damper-brace system. The damper force at the first sampling point, $f_d[1]$, is therefore zero.

3. Performance assessment

To evaluate the structural performance, different performance indices, such as interstory drift and base shear force, may be defined first and subsequently used. The response reduction of the structure before and after installing the damper-brace systems can therefore be calculated by comparing its performance indices with the indices of the original structure without additional damping devices.

3.1 Minimization of interstory drift

In order to define the response parameter in terms of interstory drift, the average of root-mean-square (*rms*) of the interstory drift of the structure is used as the first performance index:

$$PI_D = \frac{1}{n}\sum_{i=1}^{n} rms\left(\delta_i\right) \quad \textit{for n-story structures} \tag{17}$$

where $\delta_i = x_i - x_{i-1}$ is the interstory drift of the i-th story in a MDOF structure, and $\delta_1 = x_1$ for the 1st floor.

To calculate the response reduction of the structure with nonlinear damper-brace systems, a response reduction index RR_D is adopted with the following form:

$$RR_D(\%) = \left(1 - \frac{PI_D}{PI_{D,org}}\right) \times 100 \tag{18}$$

where $PI_{D,org}$ is the interstory drift performance index of the original structure without the damper-brace system.

RR_D represents the percentage of the *rms* value of interstory drift that has been reduced by the supplementary damper systems, and a large response reduction index represents a more effective design of the systems. In addition, a stiffness ratio of the brace α and a damping ratio of the nonlinear damper β relative to that of the structure are defined to relate the design parameters of the damper-brace systems to the structural properties:

$$\alpha \equiv \frac{k_b}{k_s}, \quad \beta \equiv \frac{c_d}{2m_s\omega_s} \tag{19}$$

where $\omega_s = \sqrt{k_s / m_s}$ is the natural circular frequency of the structure.

The SDOF structure, as shown in Fig. 2(a), is first investigated in this section to evaluate the effects of different deign parameters on the dynamic performance of the structure. The natural period T_s, story mass m_s and story stiffness k_s of the structure are 1 second, 2533 kg and 100 kN/m, respectively. The inherent damping ratio is set as 2%, and the external excitation used is a zero-mean white noise ground acceleration. The maximum (or optimal) response reduction $RR_{D,opt}$ and the corresponding optimal damping ratio $\beta_{D,opt}$ against the brace stiffness ratio α are computed by the proposed time-stepping method for velocity exponents v equals 0.4, 0.5, 0.6, 0.8 and 1.0, as shown in Fig. 3 below:

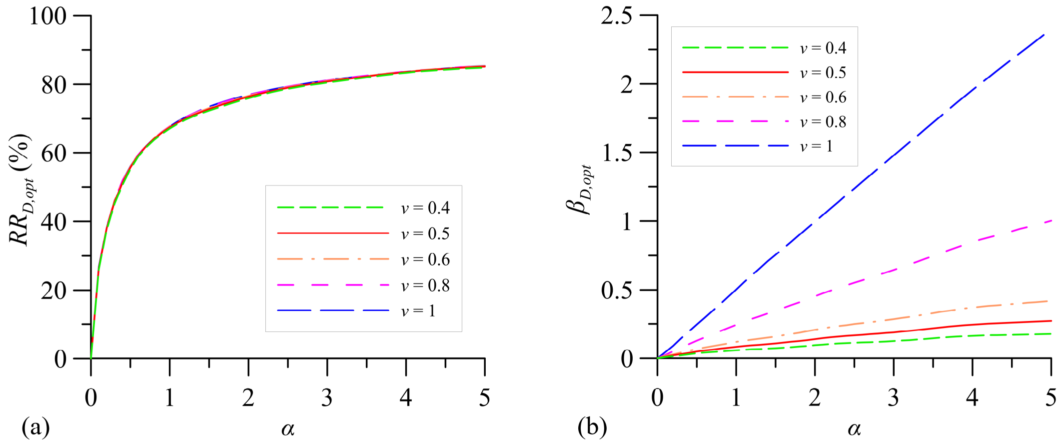

Fig. 3 – (a) Maximum response reduction $RR_{D,opt}$ and (b) corresponding optimal damping ratio $\beta_{D,opt}$ versus brace stiffness ratio α for SDOF structure under white noise

It can be seen from Fig. 3(a) that, the maximum response reduction of interstory drift increases rapidly with increasing brace stiffness when stiffness ratio α is less than 1, which means that this optimal response reduction is highly sensitive to the brace stiffness when the stiffness ratio is small, and a slight increase in brace stiffness can improve the optimal performance of the damper significantly. However, when the stiffness ratio α is larger than 1, the growth in the maximum response reduction reduces. Moreover, the maximum response reduction changes slightly for different velocity exponent v, which indicates that if there is no constraint on damping coefficient, the effect of velocity exponent is insignificant on the optimal interstory drift response. It can also be observed from Fig. 3(a) that, when a target response reduction is set, there exists a minimum brace stiffness to achieve the desired response reduction. The required optimal damping ratios for achieving the maximum interstory drift response reduction against the brace stiffness ratio are shown in Fig. 3(b). It can be seen from Fig. 3(b) that, the optimal damping ratios for interstory drift are nearly linear with the brace stiffness, regardless of the value of nonlinear velocity exponent. It can also be seen from Fig. 3(b) that, compare with linear dampers, a velocity exponent v less than 1 can reduce a considerable amount of the required damping to achieve the optimal performance. For instance, when α equals 1, i.e. brace stiffness equals story stiffness, the required damping ratio for the optimal interstory drift performance reduces from 0.50 to 0.24 as the velocity exponent v decreases from 1 to 0.8.

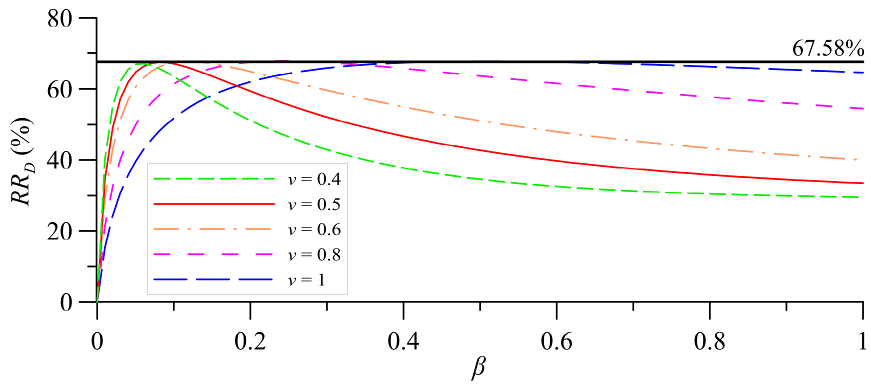

Fig. 4 – Variation of interstory drift response reduction RR_D with damping ratio β for different velocity exponents v when stiffness ratio α equals 1

Fig. 4 shows the variation of response reduction of interstory drift with damping ratio β for different velocity exponents as stiffness ratio equals the story stiffness. It can be seen from Fig. 4 that, the maximal response reduction (peak values of RR_D) for all velocity exponents are almost the same. This agrees well with the observation from Fig. 3, which shows that the maximum response reduction only changes slightly for different nonlinear velocity exponent v if no constraint on damping coefficient. Fig. 4 also shows that, to achieve a certain target response reduction, there exist many possible combinations of design parameters, e.g.

when α is equal to 1, the damping ratio β can be 0.04 and 0.19 for v equals 0.5, or 0.09 and 0.68 for v equals 0.8, or other values that can be read from Fig. 4, to achieve a 60% response reduction.

3.2 Minimization of base shear

In addition to the interstory drift performance index, the *rms* of base shear V_s of the structure may also be used as the second performance index:

$$PI_V = rms(V_s) \tag{20}$$

The corresponding response reduction for base shear RR_V can be expressed as:

$$RR_V(\%) = \left(1 - \frac{PI_V}{PI_{V,org}}\right) \times 100 \tag{21}$$

where $PI_{V,org}$ is the base shear performance index of the original structure without the damper-brace system.

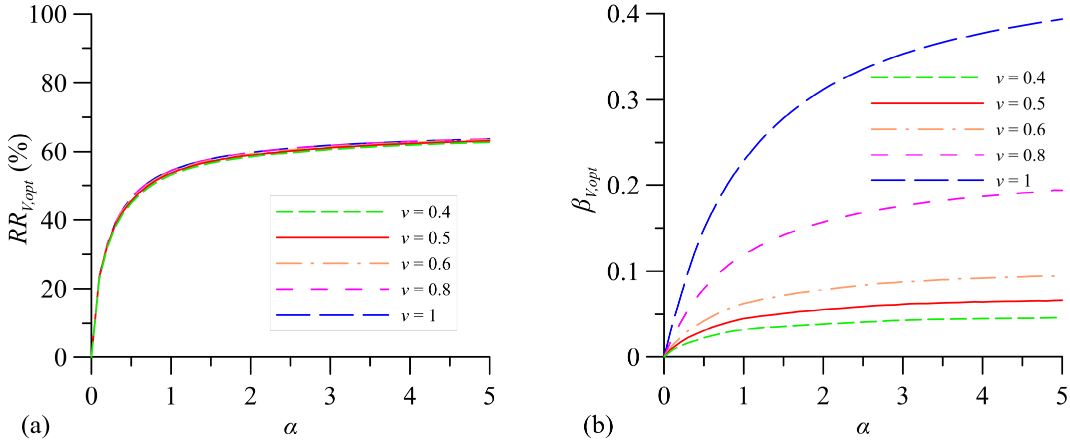

Fig. 5 – (a) Maximum response reduction $RR_{V,opt}$ and (b) corresponding optimal damping ratio $\beta_{V,opt}$ versus brace stiffness ratio α for SDOF structure under white noise

The same SDOF structure used in Section 3.1 is studied for finding the optimal base shear response reduction $RR_{V,opt}$ and the corresponding design parameters. The plots of $RR_{V,opt}$ and the optimal damping ratio $\beta_{V,opt}$ versus the brace stiffness ratio α for velocity exponents v equals 0.4, 0.5, 0.6, 0.8 and 1.0 are shown in Fig. 5. It can be observed from Fig. 5(a) that, similar to the case for interstory drift, if there is no constraint on damping coefficient, the maximum base shear response reduction also shows a sharp increase with brace stiffness when the stiffness ratio is smaller than one, and a diminishing return can be found in the large brace stiffness region. Moreover, for a given response reduction, similar to the case for interstory drift response reduction, there also exists a minimum brace stiffness; and the velocity exponent has very limited effect on the maximum base shear performance reduction, as the response reduction curves for different velocity exponents are relatively close to each other. It can be seen from Fig. 5(b) that, unlike the interstory drift case, the curves are nonlinear, and a smaller damper exponent requires less damping to reach the same performance reduction. Furthermore, if the velocity exponent is preset, for a given brace stiffness, there exists a unique optimal damping coefficient of the damper.

4. Analytic model for a MDOF structure with nonlinear damper-brace systems

The numerical time-stepping method developed in Section 2 for calculating the response history of a SDOF structure will now be extended to MDOF structures. The equation of motion of a n-degree-of-freedom structure controlled by n nonlinear FVDs installed on Chevron braces can be described as:

$$\mathbf{M_s}\ddot{\mathbf{x}}_\mathbf{s}(t) + \mathbf{C_s}\dot{\mathbf{x}}_\mathbf{s}(t) + \mathbf{K_s}\mathbf{x_s}(t) + \mathbf{F_d}(t) = -\mathbf{M_s}\mathbf{1}\ddot{x}_g(t) \tag{22}$$

where

$$\mathbf{F_d}(t)=\begin{bmatrix} f_{d,1}(t)-f_{d,2}(t) \\ f_{d,2}(t)-f_{d,3}(t) \\ \vdots \\ f_{d,n-1}(t)-f_{d,n}(t) \\ f_{d,n}(t) \end{bmatrix} \tag{23}$$

and $f_{d,i}(t)$ is the force in the nonlinear damper-brace system that installed at i-th floor; if no damper is installed, damper force in that floor should be zero. $\mathbf{M_s}$, $\mathbf{C_s}$ and $\mathbf{K_s}$ are the $n \times n$ mass, damping and stiffness matrices of the inherent structure, respectively, $\mathbf{x_s}(t)$ is the $n \times 1$ story displacement vector and $\mathbf{1}=[1 \ \ \cdots \ \ 1]^{\mathrm{T}}$ is the $n \times 1$ unit vector.

The equation of motion can be expressed by a first order differential equation:

$$\dot{\mathbf{z}}(t)=\mathbf{A}^*\mathbf{z}(t)+\mathbf{B}^*\mathbf{F_d}(t)+\mathbf{E}^*\ddot{x}_g(t) \tag{24}$$

where $\mathbf{z}(t)=\begin{bmatrix} \mathbf{x_s}(t) \\ \dot{\mathbf{x}}_\mathbf{s}(t) \end{bmatrix}$ is the $2n \times 1$ response vector, $\mathbf{A}^*=\begin{bmatrix} \mathbf{0} & \mathbf{I} \\ -\mathbf{M_s^{-1}K_s} & -\mathbf{M_s^{-1}C_s} \end{bmatrix}$ is the $2n \times 2n$ system matrix, $\mathbf{B}^*=\begin{bmatrix} \mathbf{0} \\ -\mathbf{M_s^{-1}} \end{bmatrix}$ is the $2n \times n$ damper force distribution matrix, $\mathbf{E}^*=\begin{bmatrix} \mathbf{0} \\ \mathbf{M_s^{-1}E} \end{bmatrix}$ is the $2n \times n$ external excitation distribution matrix and $\mathbf{E}=-\mathbf{M_s 1}$.

The assumptions made in Section 2.1 about damper force and external ground acceleration between two consecutive sampling instants are still valid; hence, the discrete time-state function of the structural response under a ground acceleration $\ddot{x}_g(t)$ can be described as:

$$\mathbf{z}[k+1]=\mathbf{A_e z}[k]+\mathbf{B_e F_d}[k]+\mathbf{E_0}\ddot{x}_g[k]+\mathbf{E_1}\ddot{x}_g[k+1] \tag{25}$$

and the corresponding parameter matrices, namely $\mathbf{A_e}$, $\mathbf{B_e}$, $\mathbf{E_0}$ and $\mathbf{E_1}$, are the same as those listed in Section 2.1.

The calculation of the next step structural response $\mathbf{z}[k+1]$ in Eq. (25) requires the damper force in step k to be known. The damper force $f_{d,i}[k]$ at i-th floor can be calculated first using Eq. (16), followed by assembling the damper force at each floor into Eq. (23) to form the damper force vector $\mathbf{F_d}[k]$.

5. Numerical example

The proposed time-stepping method for MDOF structures will now be demonstrated using a 2-story shear-type building with two supplementary damper-brace systems installed at each floor. The two story building structure is the same as that studied by Lavan and Levy [19], and the inherent damping ratio of the structure is assumed to be 3% for the two modes of vibration. The fundamental periods of the building are 0.281 and 0.115 seconds, and the ground acceleration in this example is the same white-noise used in Section 3. The mass and stiffness matrices of the building are:

$$\mathbf{M_s}=\begin{bmatrix} 25000 & 0 \\ 0 & 25000 \end{bmatrix}(\text{kg}) \quad \text{and} \quad \mathbf{K_s}=\begin{bmatrix} 62500 & -25000 \\ -25000 & 25000 \end{bmatrix}(\text{kN/m}) \tag{26}$$

The proposed method in Section 4 can be used to compute the performance index for interstory drift of the structure under the white noise excitation. The corresponding response reduction RR_D, can therefore be calculated for different design parameters. The objective of this example is to find the combinations of damping coefficients of the nonlinear damper at 1st story c_{d1} and the damper at 2nd story c_{d2} to achieve a maximal interstory drift response reduction $RR_{D,opt}$ for different brace stiffness ratios and velocity exponents.

Fig. 6(a) shows the maximum response reduction of interstory drift versus brace stiffness for different velocity exponents, while Fig. 6(b) and (c) show respectively the optimal damping coefficients $c_{d1,opt}$ and $c_{d2,opt}$ versus the brace stiffness for different velocity exponents. It can be seen from Fig. 6(a) that, curves similar to those in Fig. 3(a) for SDOF structure, are observed. The maximum response reduction, if no constraint is set on the damping coefficients, increases rapidly at small brace stiffness range; but this increase becomes gradual when the brace stiffness is large. It can also be seen from Fig. 6(a) that, the change of damper exponent has an indistinctive effect on the optimal interstory drift performance of the 2DOF structure. It can be observed from Fig. 6(b) and (c) that, in general, the use of a large brace stiffness requires larger damping coefficients, and the use of a small velocity exponent results in smaller optimal damping coefficients, for both dampers. To better illustrate the variation of response reduction with two damping coefficients, an exhaustive search is also conducted. Fig. 6(d) shows the exhaustive search result of a three-dimensional plot of response reduction versus two damping coefficients c_{d1} and c_{d2} with the velocity exponent equals 0.5 and the brace stiffness equals the first story stiffness. It can be seen from the Fig. 6(d) that, for a give brace stiffness and a nonlinear velocity exponent, there exists a maximum response reduction in interstory drift, and the two corresponding damping coefficients are the optimal ones for the two dampers.

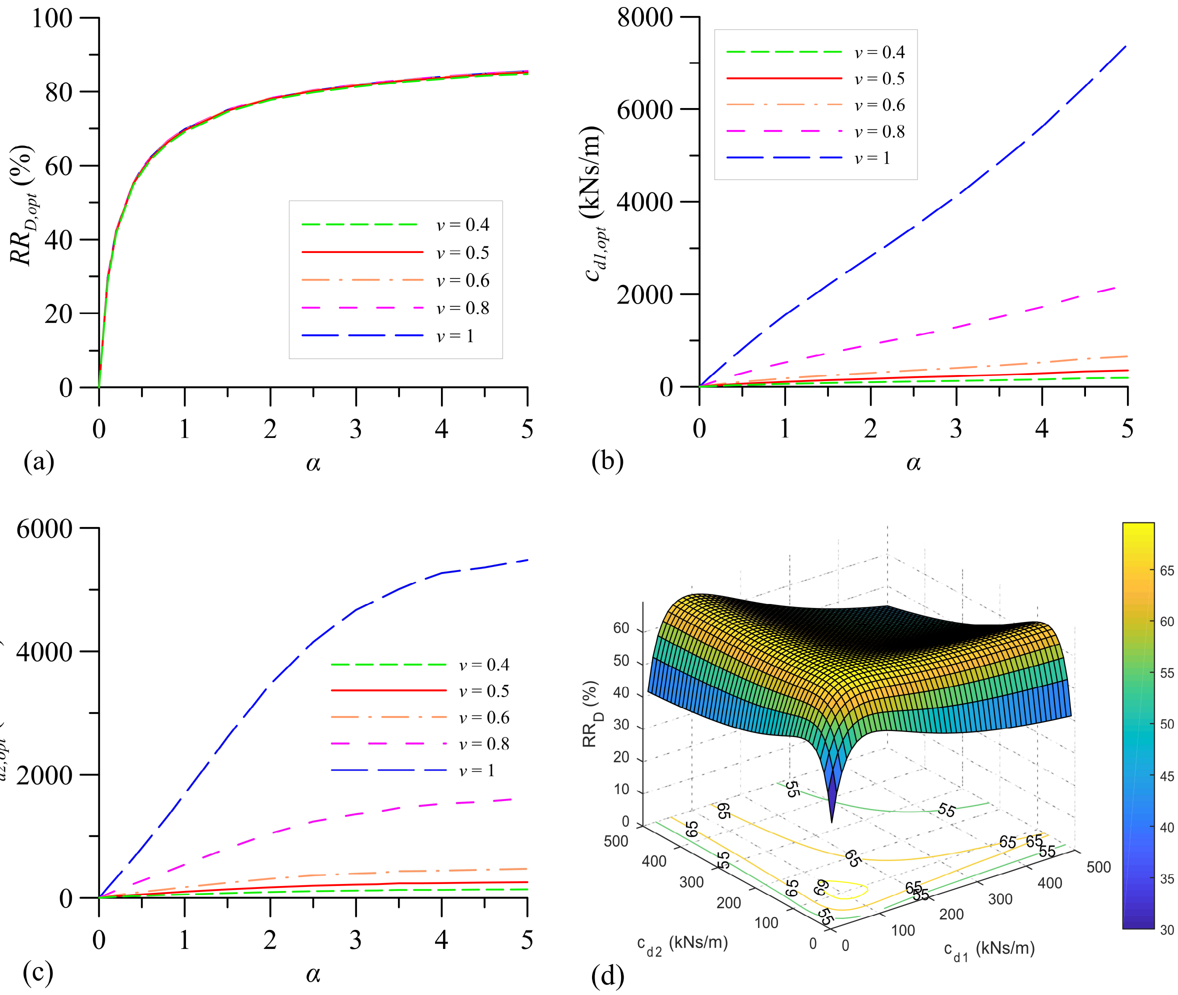

Fig. 6 – (a) Maximum response reduction versus brace stiffness ratio; (b) optimal damping coefficient of the damper at 1st story versus brace stiffness ratio; (c) optimal damping coefficient of the damper at 2nd story versus brace stiffness ratio; (d) Response reduction versus two damping coefficients (α = 1, v = 0.5)

6. Conclusion

In this paper, a procedure to design a shear-type building with braces and nonlinear fluid viscous dampers for achieving a target performance is proposed. A numerical time-stepping method to obtain the dynamic response of a SDOF structure with a nonlinear damper-brace system subjected to external excitations is first developed. Two performance indices, namely interstory drift and base shear force, are defined as the basis for the optimization of structural response. Optimal design parameters of the nonlinear damper and brace for achieving a maximal structural response reduction can then be found. Effects of different design parameters on the overall performance of a SDOF structure with a damper-brace assembly are also investigated. The results indicate that, there exist many combinations of design parameters for the nonlinear damper-brace system to reach a set performance objective; however, if no constraint is set on the damping coefficient of the damper, there exists a minimum brace stiffness for the system to achieve the desired structural performance. Moreover, once the velocity exponent of the damper is preset, for a given brace stiffness, the optimal damping coefficients can be uniquely determined. For the design of supporting braces, results show that, when the stiffness is less than the story stiffness, a small increase in brace stiffness can improve the optimal performance of dampers as well as the optimal structural performance significantly; however, when the stiffness is larger than the story stiffness, the increase in brace stiffness has limited impact on the maximum structural response reduction. Results also indicate that, the use of a nonlinear damper with a velocity exponent less than 1 can save a considerable amount of damping originally required by a linear damper to achieve a similar structural performance. The proposed procedure is easily extendable to multistory structures with multiple nonlinear damper-brace systems, as has been shown in the case study of a 2-story shear building.

7. Acknowledgements

This research is supported by Ningbo Natural Science Program (2018A610352) and Faculty Inspiration Grant.

8. References

[1] Soong TT, Spencer Jr BF (2002): Supplemental energy dissipation: state-of-the-art and state-of-the-practice. *Engineering Structures*, **24** (3), 243-259.

[2] Constantinou MC, Symans MD (1992): Experimental and analytical investigation of seismic response of structures with supplemental fluid viscous dampers. *Technical Report NCEER-92-0032*, National Center for Earthquake Engineering Research, Buffalo, USA.

[3] Tsopelas P, Okamoto S, Constantinou MC, Ozaki D, Fujii S (1994): NCEER-Taisei Corporation research program on sliding seismic isolation systems for bridges: Experimental and analytical study of systems consisting of sliding bearings, rubber restoring force devices and fluid dampers. *Technical Report NCEER-94-0002*, National Center for Earthquake Engineering Research, Buffalo, USA.

[4] Reinhorn AM, Li C, Constantinou MC (1995): Experimental and analytical investigation of seismic retrofit of structures with supplemental damping: Part.1-fluid viscous damping devices. *Technical Report NCEER-95-0001*, National Center for Earthquake Engineering Research, Buffalo, USA.

[5] Hwang JS, Huang YN, Hung YH (2005): Analytical and experimental study of Toggle-Brace-Damper systems. *Journal of Structural Engineering*, **131** (7), 1035-1043.

[6] De Domenico D, Ricciardi G (2019): Earthquake protection of structures with nonlinear viscous dampers optimized through an energy-based stochastic approach. *Engineering Structures*, **179**, 523-539.

[7] Lin WH, Chopra AK (2002): Earthquake response of elastic SDF systems with non-linear fluid viscous dampers. *Earthquake Engineering and Structural Dynamics*, **31** (9), 1623-1642.

[8] Taylor DP (2010): History, design, and applications of fluid dampers in structural engineering. Retrieved June 16, 2019, from *https://www.taylordevices.com/wp-content/uploads/68-History-Design-Application.pdf*.

[9] Tubaldi E, Kougioumtzoglou IA (2015): Nonstationary stochastic response of structural systems equipped with nonlinear viscous dampers under seismic excitation. *Earthquake Engineering and Structural Dynamics*, **44** (1), 121-138.

[10] Altieri D, Tubaldi E, De Angelis M, Patelli E, Dall'Asta A (2018): Reliability-based optimal design of nonlinear viscous dampers for the seismic protection of structural systems. *Bulletin of Earthquake Engineering*, **16** (2), 963-982.

[11] Xie Y, Zhang J, Xi W (2018): Effectiveness evaluation and optimal design of nonlinear viscous dampers for inelastic structures under pulse-type ground motions. *Earthquake Engineering and Structural Dynamics*, **47** (14), 2802-2820.

[12] Moslehi Tabar A (2019): Linearization of seismic response of structures equipped with nonlinear viscous dampers using perturbation technique. *Engineering Structures*, **184**, 459-468.

[13] Park JH, Kim J, Min KW (2004): Optimal design of added viscoelastic dampers and supporting braces. *Earthquake Engineering and Structural Dynamics*, **33** (4), 465-484.

[14] Takewaki I, Yoshitomi S (1998): Effects of support stiffnesses on optimal damper placement for a planar building frame. *Structural Design of Tall Buildings*, **7** (4), 323-336.

[15] Huang HC (2009): Efficiency of the motion amplification device with viscous dampers and its application in high-rise buildings. *Earthquake Engineering and Engineering Vibration*, **8** (4), 521-536.

[16] Londoño JM, Neild SA, Wagg DJ (2013): A noniterative design procedure for supplemental brace-damper systems in single-degree-of-freedom systems. *Earthquake Engineering and Structural Dynamics*, **42** (15), 2361-2367.

[17] Chen YT, Chai YH (2011): Effects of brace stiffness on performance of structures with supplemental Maxwell model-based brace-damper systems. *Earthquake Engineering and Structural Dynamics*, **40** (1), 75-92.

[18] Lu LY, Lin GL, Shih MH (2012): An experimental study on a generalized Maxwell model for nonlinear viscoelastic dampers used in seismic isolation. *Engineering Structures*, **34**, 111-123.

[19] Lavan O, Levy R (2006): Optimal design of supplemental viscous dampers for linear framed structures. *Earthquake Engineering and Structural Dynamics*, **35** (3), 337-356.

